VLSI DESIGN
1998, Vol. 8, Nos. (1–4), pp. 437–442
Reprints available directly from the publisher
Photocopying permitted by license only

Study on Possible Double Peaks in Cutoff Frequency Characteristics of AlGaAs/GaAs HBTs by Energy Transport Simulation

T. OKADA and K. HORIO*

Department of Electronic Information Systems, Faculty of Systems Engineering, Shibaura Institute of Technology, 307 Fukasaku, Omiya 330, Japan

By using an energy transport model, we simulate cutoff frequency f_T versus collector current density I_C characteristics of npn^-n AlGaAs/GaAs heterojunction bipolar transistors (HBTs) with various n^--collector thickness and n^--doping densities. It is found that the calculated f_T characteristics show double peak behavior when the n^--layer is thick enough and the n^--doping is high enough to allow existence of neutral n^--region. The mechanism of the double peak behavior is discussed by studying energy band diagrams, electron-energy profiles and electron-velocity profiles. Particularly, we discuss the origin of the second peak (at higher I_C) which is not usually reported experimentally.

Keywords: GaAs, heterojunction bipolar transistor, energy transport model, cutoff frequency, double peaks, velocity overshoot

1. INTRODUCTION

Recently, AlGaAs/GaAs heterojunction bipolar transistors (HBTs) have received great interest for application to high-speed and high-frequency devices. Since non equilibrium carrier transport becomes important in the HBTs, carrier energy should be considered in the modeling of them. For this purpose, the Monte Carlo simulation [1, 2] and so-called an energy transport model [3–7] have been applied to analyze the characteristics of AlGaAs/GaAs HBTs.

Cutoff frequency f_T is one of the figure-of-merits of HBTs' high-frequency performance. Usually, the cutoff frequency of AlGaAs/GaAs HBTs increases with the collector current density I_C and begins to decrease at a certain I_C, showing a single peak in the experimental $f_T - I_C$ characteristics. However, according to the simulation using a drift-diffusion model, the $f_T - I_C$ characteristics show a steep second peak in some cases [5, 8]. This is attributed to the fact that in the drift-diffusion approximation, electron mobility is given as a function of *local* electric field and the electron

* Corresponding author: Fax: +81-48-687-5198, e-mail: horio@sic.shibaura-it.ac.jp.

velocity versus electric field curve of GaAs shows a peak behavior. By the other simulation methods, the second peak has not been reported yet.

In this work, we have systematically and carefully analyzed the f_T characteristics of AlGaAs/GaAs HBTs by using an energy transport model [9] in which electron mobility is determined by an electron energy (not by local electric field) and velocity overshoot can be treated. As a result, we have found that the second peak can arise (at rather high current levels) also when using this model. Therefore, we discuss here the physical reason why the double peak behavior in the f_T characteristics arises.

2. PHYSICAL MODEL

2.1. Device Structure and Basic Equations

Figure 1 shows an npn^-n AlGaAs/GaAs HBT structure analyzed here. Al composition changes from 0.3 to 0 in the emitter and base regions, and so this is a graded band-gap base HBT. Doping densities are different in respective regions, and hence in general, transport parameters should be given as functions of Al composition, doping density and carrier energy. We have simulated the device characteristics as parameters of n^--collector thickness L_{C1} and its doping density N_{C1}.

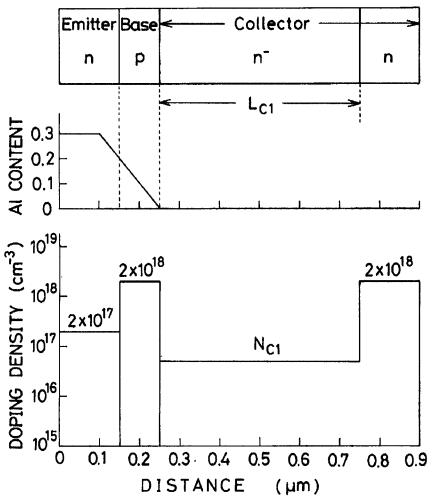

FIGURE 1 AlGaAs/GaAs HBT structure simulated in this study.

Next we describe the derivation of electron transport equations. Assuming parabolic energy bands, three conservation equations, that is, a particle conservation equation, a momentum conservation equation and an energy conservation equation are obtained by taking moments of the Boltzmann equation [10]. To make these equations tractable and applicable to the HBTs, the following assumptions are made [5]. Firstly, we adopt relaxation time approximation for collision terms. Secondly, we adopt an equivalent one-valley model. If we assume that electron drift energy is negligible small as compared to its thermal energy, the average electron energy w_n can be written as

$$w_n = \frac{3}{2} k T_n + F_U \Delta_{LU} \tag{1}$$

where T_n is electron temperature, F_U is upper-valley fraction and Δ_{LU} is energy difference between upper and lower valleys. To treat HBTs, some factors are also considered. Carrier recombination is treated by SRH statistics, and an effective field acting on electrons which arises due to the position dependence of band structure is included. Then the electron transport equations are simplified as follows.

$$\frac{dJ_n}{dz} = q U \tag{2}$$

$$J_n = -qnv_n = q\mu_n(w_n)\left\{ n E_n + \frac{d}{dz}\left(n \frac{k T_n}{q} \right) \right\} \tag{3}$$

$$-\frac{d}{dz}\left\{ \frac{J_n}{q} (w_n + kT_n) \right\} = J_n E_n - w_n U - n \frac{w_n - w_0}{\tau_w} \tag{4}$$

where U is the recombination rate, v_n is the average electron velocity, μ_n is the electron mobility, E_n is the effective field acting on electrons, τ_w is the energy relaxation time and w_0 is the equilibrium value of w_n. In the electron transport equations, parameters that should be given are

the electron mobility μ_n, the energy relaxation time τ_w and the upper-valley fraction F_U.

For holes, we use drift-diffusion type equations. In addition to the transport equations, we include Poisson's equation, which completes the basic equations for device simulation.

2.2. Transport Parameters

Here we describe methods of giving transport parameters such as μ_n, τ_w and F_U. To do this, usually, homogeneous bulk is assumed ($d/dz = 0$). Then, the following two equations are obtained from the previous electron transport equations.

$$v_n = -\mu_n E \tag{5}$$

$$w_n = w_0 - q\tau_w v_n E \tag{6}$$

where E is electric field. By using the Monte Carlo method, v_n, w_n and F_U are obtained as a function of electric field E. Thus, by using Eqs. (5) and (6), the energy-dependent μ_n, τ_w and F_U can be obtained.

In this work, we must give the transport parameters as functions of Al composition x, electron energy w_n and doping density N. To do this, we first evaluate μ_n, τ_w and F_U for $x = 0$, 0.05, 0.1, 0.15, 0.2, 0.25 and 0.3 by a Monte Carlo method. Doping densities are also varied. Once these parameters are available as fit curves or tables for a given doping density, parameters for any x between 0 and 0.3 can be obtained (as a function of w_n) by a linear extraporation method. That is, if x lies between x_1 and x_2, the parameter f is given by the following equation.

$$f(w_n) = f_1 + \frac{x - x_1}{x_2 - x_1}(f_2 - f_1) \tag{7}$$

where f_1 and f_2 are corresponding values of f for $x = x_1$ and x_2, respectively.

Next we show some examples of transport parameters estimated by a Monte Carlo method. Figure 2 shows electron mobility μ_n, energy relaxation time τ_w and upper valley fraction F_U as a parameter of Al composition x. The doping density is 2×10^{18} cm^{-3}. Here, we consider L-valley as upper valley and use L-valley's parameters for Δ_{LU} and upper-valley effective mass. We also treat a case somewhat considering X-valley's contribution, but x and energy dependences of estimated parameters are essentially similar to those shown in Figure 2 [9]. As described before, once the figures like Figure 2 are obtained for a given doping density, the transport parameters for any x and for any electron energy are obtained by the linear extraporation method. Of course, when the doping density becomes different, another figure is required. Furthermore, the parameters must be evaluated in every mesh point. However, this approach is simple in itself and can be easily implemented.

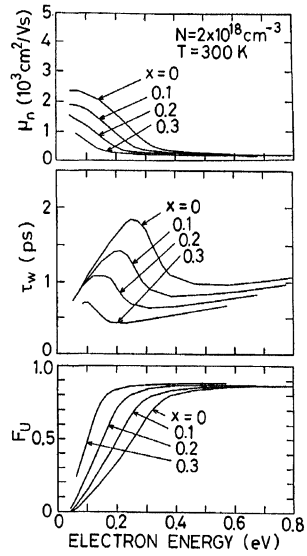

FIGURE 2 Electron mobility μ_n, energy relaxation time τ_ω and upper-valley fraction F_U versus electron energy ω_n curves as a parameter of x in $Al_xGa_{1-x}As$, calculated by a Monte Carlo method. The energy difference between upper and lower valleys Δ_{LU} and upper-valley effective mass m_U are set to $0.284-0.605x$ (eV) and $0.23\,m_0$, respectively.

3. SIMULATED $f_T - I_C$ CHARACTERISTICS

We calculate $f_T - I_C$ characteristics of the AlGaAs/GaAs HBT as parameters of the n^- collector

thickness L_{C1} and its doping density N_{C1}. Here f_T is calculated from the following equation.

$$f_T = (1/2\pi)(\partial I_C/\partial Q_n)_{V_{CE}} \quad (8)$$

where Q_n is electron charges in the device and V_{CE} is the collector-emitter voltage. V_{CE} is set to 1.5 V in this study.

Figure 3 shows calculated $f_T - I_C$ characteristics of the HBT as a parameterof n^--layer doping density N_{C1}, where L_{C1} is set to 0.5 μm. Figure 4 shows calculated $f_T - I_C$ characteristics of the HBT as a parameter of n^--layer thickness L_{C1}, where N_{C1} is set to 5×10^{16} cm^{-3}. As I_C increases, f_T increases because the emitter charging time and the collector charging time are reduced. From these figures, we see that for lower N_{C1} (10^{16} cm^{-3} in Fig. 3) and for thinner L_{C1} (0.1 μm and 0.2 μm in Fig. 4), f_T characteristics show a single peak. These cases correspond to the situation that n^--collector layer is almost or fully depleted already when the base-emitter voltage (V_{BE}) is 0 V. In the other cases,two peaks are clearly seen in the f_T characteristics. In these cases, neutral n^--region exists at $V_{BE} = 0$ V.

Up to the first peak, f_T is higher for higher N_{C1}, as seen from Figure 3. Also, the value of I_C where f_T begins to decrease is higher for higher N_{C1}. These are because around the peak region, the transit time through n^--collector depletion layer (which is thinner for higher N_{C1}) is dominant [5] and f_T begins to decrease due to a high injection effect which leads to expanding the depletion layer

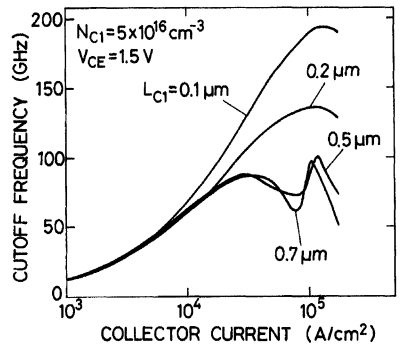

FIGURE 4 Calculated $f_T - I_C$ curves of AlGaAs/GaAs HBTs as a parameter of n^--collector thickness L_{C1}. The n^--collector doping density N_{C1} is 5×10^{16} cm^{-3}.

and increasing the collector transit time. As seen in Figure 4, the f_T characteristics are essentially similar between the two cases with $L_{C1} = 0.5$ μm and 0.7 μm. This is because the thickness of n^--collector depletion layer is determined by N_{C1}. As shown in Figure 3, when N_{C1} is higher, the value of I_C where f_T takes the second peak is higher. We will discuss below why the f_T characteristics show double peak behavior.

Figure 5 shows energy band diagrams as a parameter of I_C for the HBT where $N_{C1} = 5 \times 10^{16}$ cm^{-3} and $L_{C1} = 0.5$ μm. Figures 6 and 7 show the corresponding electron-energy profiles and electron-velocity profiles, respectively. In these figures $I_C = 10^4$ A/cm^2, 3×10^4 A/cm^2, 8×10^4 A/cm^2, 1.2×10^5 A/cm^2 and 1.5×10^5 A/cm^2 correspond to the regions before the first peak, around the first peak,

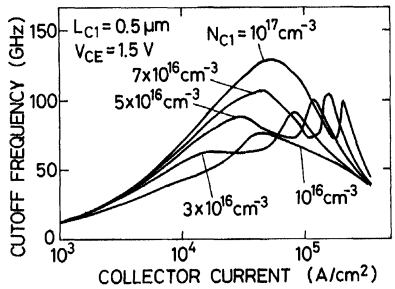

FIGURE 3 Calculated $f_T - I_C$ curves of AlGaAs/GaAs HBTs as a parameter of n^--collector doping density N_{C1}. The n^--collector thickness L_{C1} is 0.5 μm.

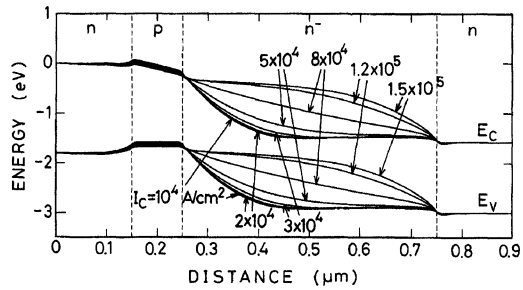

FIGURE 5 Energy band diagrams of an AlGaAs/GaAs HBT with $L_{C1} = 0.5$ μm and $N_{C1} = 5 \times 10^{16}$ cm^{-3} as a parameter of I_C. $V_{CE} = 1.5$ V.

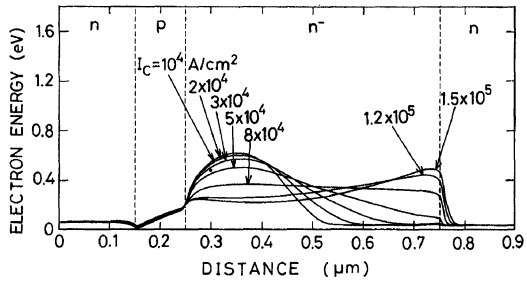

FIGURE 6 Electron-energy profiles of an AlGaAs/GaAs HBT, corresponding to Figure 5. $L_{C1}=0.5$ μm and $N_{C1}=5\times10^{16}$ cm^{-3}.

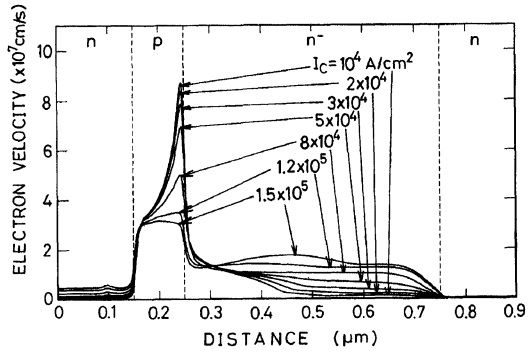

FIGURE 7 Electron-energy profiles of an AlGaAs/GaAs HBT, corresponding to Figure 5. L_{C1} = 0.5 μm and N_{C1} = 5 × 10^{16} cm^{-3}.

at the local minimum, at the second peak, and after the second peak respectively, in the f_T-I_C characteristics. From these, we interpret the double peak behavior in the following way.

As is understood from Figure 5, the first peak arises because the depletion layer in the n^--collector layer expands due to an high injection effect, and hence the collector transit time increases. The fall of I_C should last until the n^--collector layer becomes entirely depleted. Around $I_C=8\times10^4$ A/cm^2, the n^--layer is entirely depleted as seen from Figure 5 and at this current, f_T characteristics show the local minimum. As can be seen from the band diagrams, the electric field at the n^--collector layer near the base becomes weaker when I_C increases further. Hence, as shown in Figure 6, the electron energy in this region becomes lower. Consequently, the electron mobility becomes high, leading to the higher electron velocity than the saturation velocity, for example, at $I_C=1.2\times10^5$ A/cm^2 as shown in Figure 7. Therefore, the collector transit time becomes shorter temporarily and hence f_T begins to increase again. In the end, however, f_T falls because of the base-push-out effect (Kirk effect) which leads to a lower electron velocity around the base-collector interface and higher collector capacitance due to the injected electrons whose densities become higher than N_{C1}. Thus the second peak arises. As is evident from the above discussion, the value of I_C where f_T shows a second peak becomes higher for higher N_{C1}.

As described above, we have shown theoretically that double peak behavior can be seen in the f_T-I_C characteristics of AlGaAs/GaAs HBTs. Physical mechanism of this behavior has been explained.

4. CONCLUSION

By using an energy transport model, we have simulated f_T-I_C characteristics of AlGaAs/GaAs HBTs with various n^--collector thickness and n^--doping densities. It is found that the calculated f_T characteristics show the double peak feature when the n^--layer is thick enough and the n^--doping is high enough to allow existance of the neutral n^--region. It is interpreted that the first peak arises because the depletion region in the n^--layer begins to expand due to a high injection effect and the collector transit time increases. The fall of f_T lasts until the n^--layer becomes entirely depleted. When the base voltage is raised further, the electric field in the n^--layer near the base becomes lower, leading to the lower electron energy there. Then, the electron velocity in the n^--layer becomes higher, resulting in shorter collector transit time. Therefore, f_T begins to increase again. Finally, f_T decreases due to the base-push-out effect (Kirk effect), resulting in the second peak. We can say that the double peak behavior can be seen in the f_T

characteristics of real AlGaAs/GaAs HBTs if the collector current is raised rather high.

References

[1] Tomizawa, K., Awano, Y. and Hashizume, N. (1984). "Monte Carlo simulation of AlGaAs/GaAs heterojunction bipolar transistors", *IEEE Electron Device Lett.*, **EDL-5**, 362–364.

[2] Katoh, R., Kurata, M. and Yoshida, J. (1989). "Self-consistent particle simulation for (AlGa)As/GaAs HBT's with improved base-collector structures", *IEEE Trans. Electron Devices*, **36**, 846–853.

[3] Horio, K. and Yanai, H. (1987). "Numerical modeling of energy transport effects in AlGaAs/GaAs heterojunction bipolar transistors", *Proceedings of NASECODE V*, pp. 231–236.

[4] Azoff, E. M. (1989). "Energy transport numerical simulation of graded AlGaAs/GaAs heterojunction bipolar transistors", *IEEE Trans. Electron Devices*, **36**, 609–616.

[5] Horio, K., Iwatsu, Y. and Yanai, H. (1989). "Numerical simulation of AlGaAs/GaAs heterojunction bipolar transistors with various collector parameters", *IEEE Trans. Electron Devices*, **36**, 617–624.

[6] Tomizawa, K. and Pavlidis, D. (1990). "Transport equation approach for heterojunction bipolar transistors", *IEEE Trans. Electron Devices*, **37**, 519–529.

[7] Teeter, D. A., East, J. R., Mains, R. K. and Haddad, G. I. (1993). "Large-signal numerical and analytical HBT models", *IEEE Trans. Electron Devices*, **40**, 837–845.

[8] Chen, J., Gao, G. B., Unlu, M. S. and Morkoc, H. (1991). "High-frequency output characteristics of AlGaAs/GaAs heterojunction bipolar transistor for large-signal applications", *Solid-State Electron.*, **34**, 1263–1273.

[9] Nakatani, A. and Horio, K. (1995). "Energy transport modeling of HBTs considering composition-, doping- and energy-dependence of transport parameters", *Inst. Phys. Conf. Ser.*, **141**, 633–638.

[10] Blotekjaer, K. (1970). "Transport equations for electrons in two-valley semiconductors", *IEEE Trans. Electron Devices*, **ED-17**, 38–47.

Authors' Biographies

Tadayuki Okada received the M.E. degree in electrical engineering from Shibaura Institute of Technology, Japan in 1997. His research was concerned with energy transport simulation of AlGaAs/GaAs HBTs. He now works at Toshiba Information Systems Corporation, Japan. He is a member of the Japan Society of Applied Physics.

Kazushige Horio received the Ph.D. degree in electronic engineering from University of Tokyo, Japan in 1982. Now, he is a Professor at Department of Electronic Information Systems in Shibaura Institute of Technology, Japan. His research interests include modeling and simulation of high-speed and high-frequency devices such as GaAs MESFETs, HBTs and HEMTs, and simulation methods for heterojunctions and energy transport effects. He has authored more than 50 international papers in these fields. He is a senior member of IEEE and a member of the Japan Society of Applied Physics. He is listed in *Who's Who in the World.*